Photochemistry of Iodobenzene Adsorbed on Sapphire(0001)

D. Sloan, Y.-M. Sun, H. Ihm, and J. M. White*

Department of Chemistry and Biochemistry, University of Texas, Austin, Texas 78712

Received: March 17, 1998; In Final Form: June 26, 1998

Iodobenzene (C_6H_5I) dosed on sapphire(0001) at 110 K adsorbs molecularly and desorbs with a peak near 187 K, depending slightly on coverage. Irradiation with 193 nm photons induces dissociation attributable to photon absorption by C_6H_5I and C−I bond cleavage. A measurable fraction of the products are ejected during irradiation. Normalized to the initial intensities, the I XPS signal decays 2.5 times faster than the C signal. The cross sections for the loss of C_6H_5I, I, and C are $(2.8 \pm 0.3) \times 10^{-18}$, $(6.6 \pm 0.7) \times 10^{-19}$, and $(2.7 \pm 0.3) \times 10^{-19}$ cm^2, respectively. Benzene (C_6H_6) and biphenyl ($C_{12}H_{10}$) appear in TPD at temperatures consistent with desorption-limited processes.

Introduction

Many recent studies have addressed UV photochemistry of halogenated alkyl compounds adsorbed on metals and semiconductors.[1−7] In general, substrate quenching plays an important role, but because carbon−halogen bond cleavage typically occurs along a very repulsive potential energy surface, photodissociation is competitive. Metal and semiconductor substrates also supply hot carriers at the adsorbate−substrate interface which can drive substrate-mediated dissociation processes.[8−10] For alkyl halides, e.g., CH_3I[11,12] and CH_3Br,[2,13] gas-phase photodissociation involves an n → s* transition (lone pair on halogen to antibonding carbon−halogen orbital)[14,15] that cleaves the carbon−halogen bond along a steeply repulsive potential energy curve. The situation for aryl compounds is different; the longest wavelength electronic excitation involves the π electron orbitals in a $\pi \rightarrow$ p* transition followed, for dissociation, by intersystem crossing to a repulsive σ* state localized on the carbon−halogen bond, producing phenyl radicals and halogen atoms.[14−17] Toward shorter wavelengths, other excited states are formed by photon absorption, but the aryl moiety is typically involved in the photochemistry. Thus, compared to an alkyl halide, the time required for carbon−carbon bond dissociation in aryl halides is longer, and for adsorbed species, quenching is expected to be more competitive.

The aryl halide used here, C_6H_5I, dissociates in the gas phase from excited singlet states, $S_n(\pi,\pi^*)$ ($n = 1-3$), and from a repulsive triplet state, $T(\sigma,\sigma^*)$, reached by intersystem crossing.[17−19] At 248 nm, dissociation occurs from the S_1 state and produces fragments that are translationally and internally excited. However, at 193 nm dissociation occurs from the S_3 state via two distinct pathways. The first involves internal conversion from S_3 to S_1, followed by a crossover to a triplet state that produces large amounts of translational energy in the fragments. The second pathway is somewhat slower and produces fragments with less translational energy but higher internal energy in the phenyl ring. In the results reported here, the energy content of fragments is an important part of the proposed model.

The chemistry of adsorbed C_6H_5I has been examined on a wide band gap material, LiF,[1] and two metals, Cu(111)[20] and Ag(111).[21] Following adsorption on LiF at 150 K, irradiation with 222 nm pulses leads to desorption of translationally hot ($T > 1000$ K) I and C_6H_5, as well as 900 K C_6H_5I. On Ag(111) similar photodynamics experiments indicated no ejection in the first layer but translationally hot I and C_6H_5 in second and higher layers. On Cu(111), TPD results indicate that thermal dissociation leads to the formation of biphenyl, $C_{12}H_{10}$, with 100% selectivity.

Sapphire, Al_2O_3(0001), while widely used as a substrate for growing optoelectronic materials, has not been widely used as a substrate for surface chemistry studies. Any 193 nm (6.4 eV) photochemistry observed on this surface is interesting because the ∼9 eV band gap of Al_2O_3(0001) renders it transparent, except for defect state absorption. Consequently, because hot carrier substrate-mediated chemistry is negligible when compared with metals and semiconductors, the observed photochemistry must be attributed to direct absorption. In addition, electronic-state quenching rates should be relatively slow on Al_2O_3(0001), thereby allowing photodissociation channels to become more competitive.

In this paper, we describe the thermal chemistry and the X-ray and 193 nm photochemistry of C_6H_5I on Al_2O_3(0001) focusing on products retained and observed in subsequent TPD and XPS.

Experimental Section

All experiments were performed in a UHV system with a base pressure of 2×10^{-10} Torr. The system was equipped for high-resolution electron energy loss spectroscopy (HREELS), temperature-programmed desorption (TPD) and residual gas analysis (RGA), X-ray photoelectron spectroscopy (XPS), and low-energy electron diffraction (LEED). A detailed description of the system has been given elsewhere.[22] While success has been reported in dealing with charging,[23,24] we have not successfully acquired LEED or HREELS data. In XPS, charging of ∼6 eV was typical, and to account for it we forced an accepted internal standard of 531.6 eV for the O 1s binding energy (BE).[25]

The substrate, obtained from Meller Optics, was a 1× 1.5 × 0.1 cm Al_2O_3(0001) wafer polished on one side. Ta clips held it to Ta rods that were in contact with a liquid N_2 cooled Cu block. A 200 nm thick Ta film was deposited on the back of the wafer for resistive heating. The temperature was measured with a chromel−alumel thermocouple spot-welded to a small Ta clip that was glued (high-temperature ceramic adhesive) to the center of the top edge of the substrate. The sample could

S1089-5647(98)01537-5 CCC: $15.00
Published on Web 08/06/1998

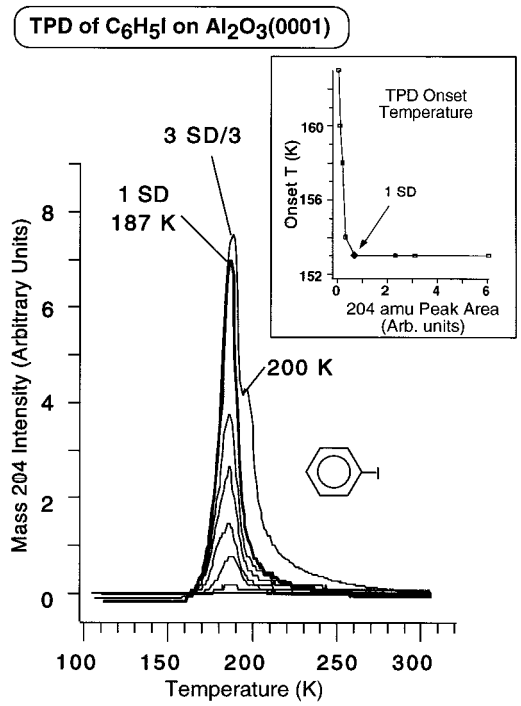

Figure 1. Mass 204 TPD spectra for C_6H_5I doses up to 3 SD on Al_2O_3-(0001) at 110 K. SD = standard dose as defined in the text. The inset plots the onset of the leading edge as a function of 204 peak area. TPD extended to 1200 K at a rate of 4 K/s. The bold curve is defined as 1 SD (see text), and its onset temperature is indicated in the inset.

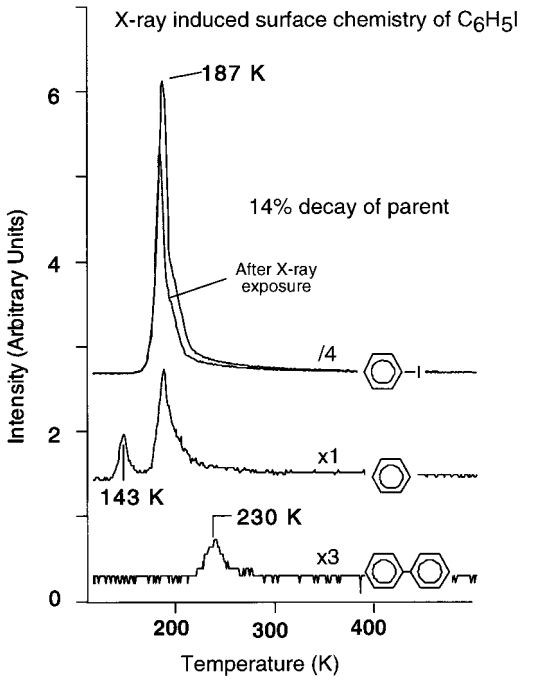

Figure 2. TPD spectra of C_6H_5I, C_6H_6, and $C_{12}H_{10}$ after 20 min X-ray exposure of 1 SD of C_6H_5I. The dashed curve is the parent TPD peak found when X-rays were not used.

be cooled to 110 K or heated, typically 4 K/s, using a dc power supply and a temperature controller. The sample was cleaned, as verified by XPS, by sputtering with 3 kV Ar^+ ions and annealing to 1000 K for 3 min, followed by flashing to 1200 K.

The quadrupole mass spectrometer (QMS) ionizer was covered by a shroud with a mesh-covered 6 mm i.d. entrance aperture. The sample was positioned, in line-of-sight, 8 cm away from the ion source filament and 2 cm from the shroud. Before dosing, the C_6H_5I was purified, as confirmed by RGA, using several freeze/pump/thaw cycles. C_6H_5I was dosed reproducibly, but without absolute calibration, using a measured pressure, typically 0.5 Torr, behind a ca. 10 μm diameter pinhole. Doses are specified in terms of a standard dose (SD), internally calibrated with respect to the characteristics of the C_6H_5I TPD (see below). In other experiments, C_6H_6, $C_{12}H_{10}$, D_2, and D_2O were purified, analyzed, and dosed in a similar manner.

For photolysis, low-energy ($\sim$1 mJ cm^{-2}) 193 nm excimer laser pulses were incident through a LiF window at an angle of $\sim$45° to the surface normal. No temperature increase was observed during irradiation.

Results

TPD. Parent 204 amu ($C_6H_5I^+$) TPD spectra obtained after several doses (no photons) of C_6H_5I at 110 K (Figure 1) are characterized by peaks at 187 and 200 K with a relatively long tail. Through control experiments, the 200 K peak was traced to desorption from nonsample surfaces (mainly the Ta clips) and the long tail to pumping speed limitations for C_6H_5I. These features are not discussed further. The 187 K peak is consistent with multilayer C_6H_5I [21,26] and moves to slightly higher T with increasing dose (up to 193 K for 6 standard doses (SD)). On the basis of the thermal profiles of other ions, all of which track 204 amu and have intensities consistent with C_6H_5I, we conclude that C_6H_5I adsorbs molecularly at 110 K and desorbs with no dissociation by 200 K.

Commonly, but not here, monolayers and multilayers are distinguishable as separate TPD peaks. The onset temperatures, determined by extrapolating ln(signal) of the leading edges versus T to the background noise level, shifts downward for low doses but then becomes constant (inset). The dose for which the onset becomes constant (bold curve) is used as an internal reference and defined as 1 SD. Higher exposures have superimposable leading edges characteristic of zero-order desorption. Further, except for the desorption due to nonsample surfaces, a 3 SD exposure gives a 3-fold area increase, indicating a linear relation (constant sticking coefficient) between dose and TPD area. The same holds true for 6 SD (not shown).

Leading edge kinetic analysis of the 1 SD spectrum yields a desorption activation energy of 11.3 $\pm$ 0.5 kcal/mol, slightly lower than that measured for C_6H_5I on Cu(111)[26] but equal to the enthalpy of vaporization of 11.4 $\pm$ 1 kcal/mol.[27]

Dissociation during XPS. In this system, X-rays were shown to activate surface reactions. For a typical analysis, XPS data were obtained by signal averaging over multiple scans for each element—10 min for I $3d_{5/2}$, 7.5 min for C 1s, 1.25 min for O 1s, and 1.25 min for Al 2p—20 min total X-ray exposure. TPD spectra (Figure 2) after 1 SD of C_6H_5I was exposed to X-rays for 20 min show clear evidence for product formation and parent loss. Benzene, C_6H_6, desorbs at 143 K and biphenyl, $C_{12}H_{10}$, at 230 K. The dashed line indicates the starting amount of C_6H_5I; the area after irradiation is 14% lower. XPS data taken after TPD to 1200 K showed no signs of I or C.

To confirm that the dissociation occurred during the XPS process, C_6H_5I was dosed at 110 K and held there for 20 min without X-ray exposure. No loss of parent signal was evident in TPD, and no benzene or biphenyl desorbed (not shown). Further, after annealing to 300 K, no C or I peaks appeared in XPS; the spectra were indistinguishable from curve A of Figure 3, i.e., clean Al_2O_3(0001).

XPS vs Coverage. The XPS results, consistent with TPD, indicate that C_6H_5I adsorbs molecularly at 110 K and that some

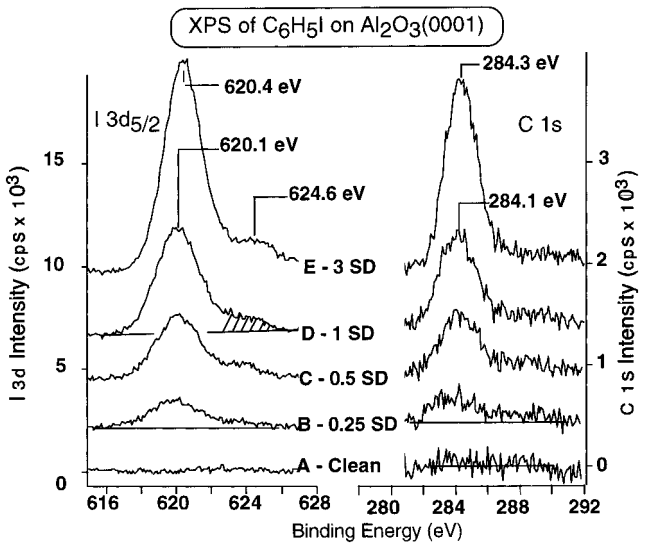

Figure 3. I $3d_{5/2}$ (left panel) and C 1s (right panel) XP spectra obtained for various doses of C_6H_5I after adsorption at a substrate temperature of 110 K. The shoulder observed in the I $3d_{5/2}$ spectra at 624.6 eV is attributed to a shake-up feature consistent with a $\pi \rightarrow$ p* transition.

X-ray-induced chemistry occurs. Figure 3 shows the I $3d_{5/2}$ and C 1s XPS of various doses, determined as described above, of C_6H_5I dosed on Al_2O_3(0001) at 110 K. The signal-to-noise level is higher for I because the atomic sensitivity factor (ASF) of I is more than an order of magnitude higher than C (I_{ASF} = 4.4, C_{ASF} = 0.205).[25] For doses up to 1 SD (spectra B−D), the I $3d_{5/2}$ peak is centered at ∼620.1 eV, as expected for molecularly adsorbed iodine-containing hydrocarbons.[5,28,29] Above 1 SD, there is a slight shift to higher BE (∼0.3 eV) in the I $3d_{5/2}$ peak for 3 SD, an effect attributable to small changes in final-state relaxation for multilayers and found on other oxides, e.g., CD_3I on TiO_2 (110).[28] Thus, the 1 SD definition is consistent with completion of the first layer of C_6H_5I.

There is a second I $3d_{5/2}$ peak at 624.6 eV (e.g., hatched region of curve D) that grows monotonically with dose which, assuming the coverage scale defined here, rules out I bonded to substrate atoms. The 4.2 eV peak separation is consistent with the energy of a $\pi \rightarrow \pi^*$ transition observed in the optical absorption spectrum of C_6H_5I.[18] Thus, this peak is attributed to a shake-up transition in C_6H_5I, i.e., simultaneous ejection of an I(3d) photoelectron and a $\pi \rightarrow \pi^*$ electronic transition.

The C 1s spectra up to 1 SD (spectra B−D) are characterized by a single peak centered at ∼284.1 eV, consistent with that observed for other aromatic compounds, i.e., simultaneous.[2,29] For 3 SD (spectrum E), there is a 0.3 eV BE increase, consistent with shifts observed for I.

XPS vs Annealing *T*. I $3d_{5/2}$ and C 1s XPS were acquired after adsorbing ∼0.33 SD C_6H_5I, annealing to various temperatures up to 400 K, and recooling for XPS. The residual C and I are removed by annealing to 1200 K. Peak areas decayed (Figure 4) in accord with the indicated TPD peaks for C_6H_6, C_6H_5I, and $C_{12}H_{10}$. Consistent with C_6H_6 desorption, annealing to 150 K lowers the C 1s but not the I $3d_{5/2}$ signal. Between 150 and 200 K, both the I $3d_{5/2}$ and C 1s peak areas decrease, qualitatively consistent with C_6H_5I desorption. The relatively strong drop of the I $3d_{5/2}$ area between 150 and 170 K requires another iodine removal channel which remains unidentified. There were no shifts in the C 1s peak position, but a slight downward shift and broadening (<0.3 eV) were observed in the I $3d_{5/2}$ peak above 200 K. The latter reflects X-ray-induced C−I bond cleavage.[5,29] About 15% of the starting C and I

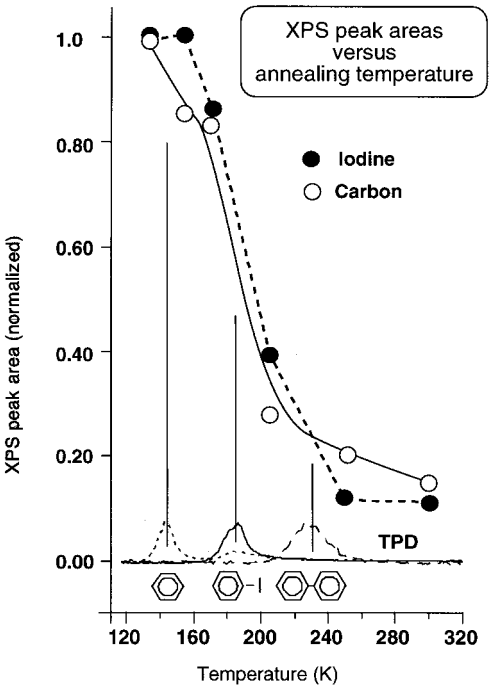

Figure 4. Decrease in the I $3d_{5/2}$ and C 1s peak areas as a function of temperature after adsorbing 0.33 SD of C_6H_5I at 110 K. The TPD spectra of C_6H_6, C_6H_5I, and $C_{12}H_{10}$ (normalized to the C_6H_5I intensity) obtained after acquiring XPS are shown at the bottom for reference.

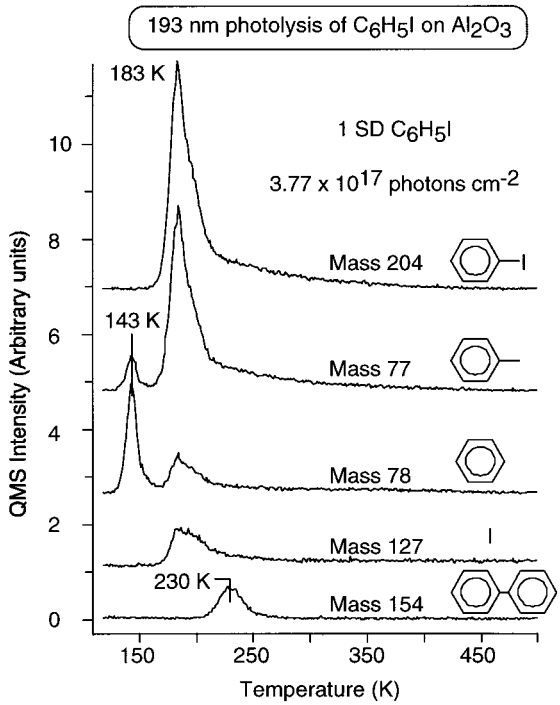

Figure 5. TPD spectra acquired after adsorbing 1 SD of C_6H_5I at a substrate temperature of 110 K and then irradiating with 3.77×10^{17} 193 nm photons/cm^2. Desorption features corresponding to C_6H_6 at 143 K and $C_{12}H_{10}$ at 230 K are observed.

remains after annealing to 400 K and is attributed to X-ray activation. This is of significance when considering the source of H to form C_6H_6.

193 nm Photon Irradiation. *TPD.* Irradiation of 1 SD with 3.77×10^{17} 193 nm photons cm^{-2} activates C_6H_5I and, as with X-ray activation, leads to C_6H_6 and $C_{12}H_{10}$ in TPD (Figure 5). The 77 and 78 amu signals are characteristic of benzene as is the peak desorption temperature verified by directly dosing

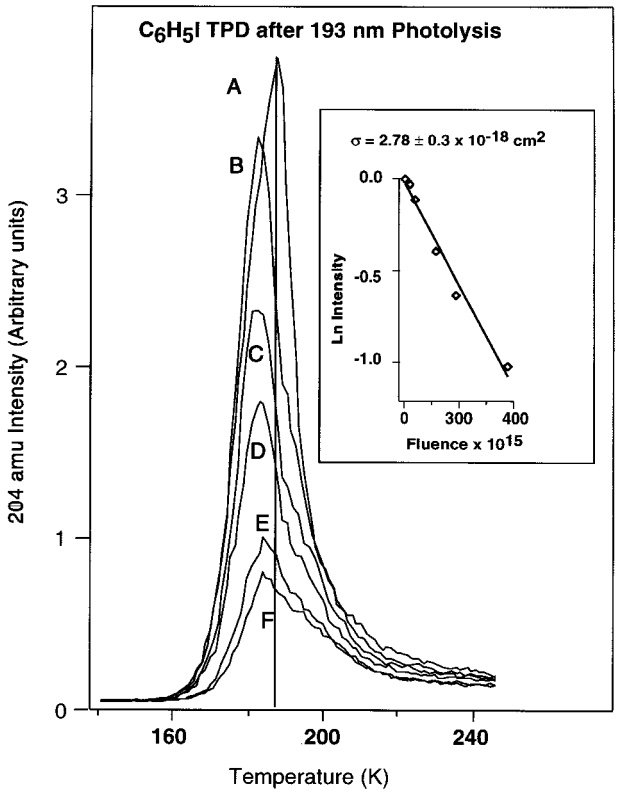

Figure 6. TPD of 204 amu after irradiating 1 SD of C_6H_5I at a substrate temperature of 110 K: (A) 0, (B) 1.88×10^{16}, (C) 3.77×10^{16}, (D) 1.13×10^{17}, (E) 1.88×10^{17}, and (F) 3.77×10^{17} photons/cm^2. The inset shows the mass 204 peak areas as a function of photon fluence. The solid line is a least-squares linear fit from which a cross section of $2.78 \pm 0.3 \times 10^{-18}$ cm^2 for the loss of C_6H_5I was obtained.

C_6H_6. Similarly, the 154 amu peak at 230 K is characteristic of dosed $C_{12}H_{10}$. All other ion signals were attributable to ion source fragmentation of C_6H_6, C_6H_5I, and $C_{12}H_{10}$; i.e., no other products were detected. In another experiment, 1 SD dosed at 110 K was irradiated at 154 K (above the C_6H_6 desorption temperature). After irradiation, TPD was recorded beginning at 110 K; no C_6H_6 desorbed while the C_6H_5I and $C_{12}H_{10}$ peak areas were within 3% of those in Figure 5.

Decay of Parent and Rise of Products. With 1 SD, the decay of the parent TPD signal with 193 nm photon fluence is shown in Figure 6. The inset plots ln(peak area) as a function of fluence, and the calculated cross section for total loss of C_6H_5I is $(2.8 \pm 0.3) \times 10^{-18}$ cm^2. Compared to curve A (no photons), the peak areas steadily decay with only a small drop in peak position ($\leq$5 K).

The intensities of the two products, C_6H_6 and $C_{12}H_{10}$, identified in Figure 5 vary with photon fluence as shown in Figure 7using the 78 amu TPD peak at 183 K and the 154 amu peak at 230 K. Both products appear in TPD from the outset of photolysis. Benzene desorption rises monotonically but nonlinearly while biphenyl reaches saturation at 4×10^{15} photons cm^{-2} and may begin to decay slightly.

For comparison, C_6H_6 and $C_{12}H_{10}$ were dosed at 110 K; the C_6H_6 TPD spectra (A, B, and C of top panel, Figure 8) have nonoverlapping leading edges, indicating that the surface coverage is not multilayer. Although the area of C is larger than D, the latter from Figure 5, the positions and shapes are coincidental showing that C_6H_6 is formed at lower temperatures, most likely during photolysis; i.e., C−I bonds are broken and C−H bonds are formed. The $C_{12}H_{10}$ TPD after photolysis is also desorption limited (lower panel of Figure 8).

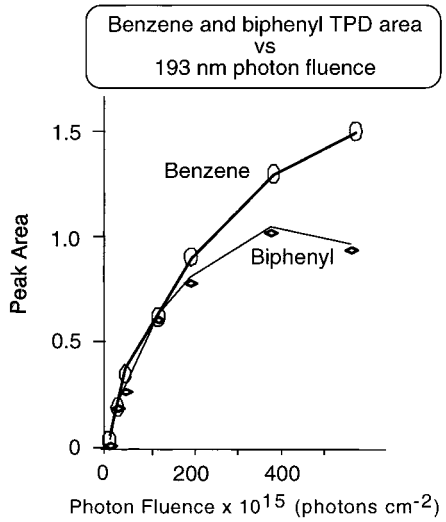

Figure 7. TPD peak areas versus 193 nm photon fluence for benzene (78 amu) and biphenyl (154 amu) produced by 193 nm irradiation of 1 SD of C_6H_5I.

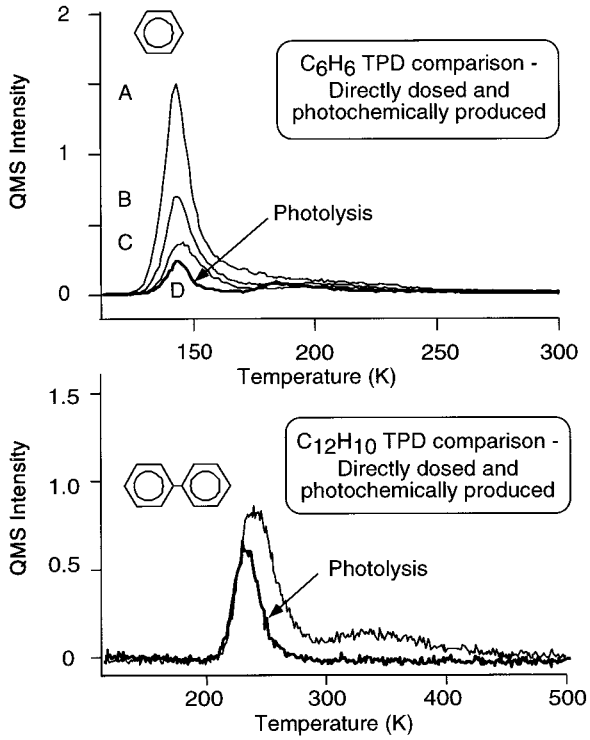

Figure 8. Top panel: spectra A, B, and C show the mass 78 TPD spectra acquired after adsorbing C_6H_6 at a substrate temperature of 110 K. Spectrum D, bold curve, taken from Figure 9 (left side), is benzene TPD after photolysis. Bottom panel: bold curve is biphenyl TPD after irradiation, and the other curve is for directly dosed biphenyl.

Source of Hydrogen To Form C_6H_6. The H source for C_6H_6 is of interest. To test background gas sources, H_2 and H_2O, we introduced D_2 and D_2O to match background amounts of H_2 and H_2O. Irradiation of 1 SD C_6H_5I in the presence of these deuterated sources led to no detectable deuterated products. Thus, hydrogen must be obtained from C_6H_5I (or its dissociation products).

Figure 4 indicates that dissociation products, formed from XPS irradiation, involve fragments that leave small amounts of carbon above the C_6H_5I and $C_{10}H_{12}$ desorption temperatures, presumably as C_xH_y or C_xH_yI. Since irradiation with 193 nm photons leads to the same TPD products, we suppose that the

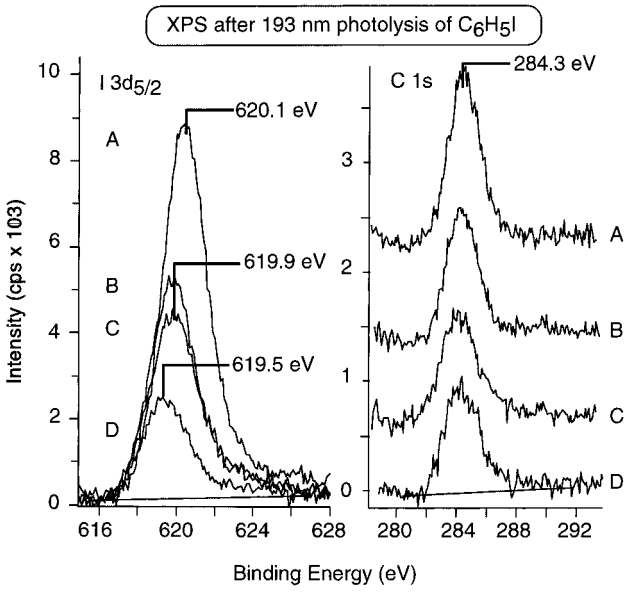

Figure 9. I $3d_{5/2}$ (left panel) and C 1s (right panel) XPS for 1 SD of C_6H_5I irradiated with (A) 0, (B) 1.88×10^{17}, (C) 3.77×10^{17}, and (D) 1.69×10^{18} 193 nm photons/cm^2.

same reactions lead to C_6H_6 and partially dehydrogenated products. Below we propose that energetic phenyl fragments formed by photodissociation of C_6H_5I abstract H from neighboring C_6H_5I to form C_6H_6 and leave C_6H_4I.

XPS after Irradiation. The loss of C and I during photolysis is indicated by decaying XPS intensities (Figure 9) as the fluence increases from 0 to 1.69×10^{18} photons cm^{-2}. Peak shifts for C 1s are negligible, but there is a measurable shift of I $3d_{5/2}$ toward lower BE (620.1 to 619.5 eV). This shift is larger than expected for a coverage change (Figure 3) and is taken to indicate a change in the chemical environment of some of the iodine due to C−I cleavage.[5,29] After a fluence of 1.69×10^{18} photons cm^{-2} (spectrum D), ~26% of the initial I $3d_{5/2}$ signal remains. Strikingly, 60% of the initial C 1s signal remains, indicating that photolysis removes a much larger fraction of the initial I than C. We were unable to observe directly the ejection of I-containing species during irradiation, but we suppose they include C_6H_5, I, and C_6H_5I as on LiF[1] and Ag(111).[21] The XPS signal decays correspond to cross sections of $(6.6 \pm 0.7) \times 10^{-19}$ and $(2.7 \pm 0.3) \times 10^{-19}$ cm^2 for the ejection of I and C, respectively. Compared to the total parent TPD loss cross section, 2.78×10^{-18} cm^2, branching ratios (ejection/retention) of ~0.31 for I atoms and ~0.11 for C atoms are obtained.

Discussion

From the foregoing results and interpretation, the following general picture emerges. Adsorption of warm (300 K) C_6H_5I on cold (110 K) Al_2O_3(0001) occurs without dissociation and with constant, probably near unity, sticking coefficient. Thermal desorption also occurs without dissociation, and monolayers and multilayers are not distinguishable on the basis of the desorption peak temperatures. The desorption onset temperature first drops with increasing dose but at a certain dose becomes constant; the latter is used to define a standard dose (SD). Coverages above this point have multilayer TPD and XPS characteristics.[5,28,29]

Photon irradiation (X-rays or 193 nm) dissociatively activates C_6H_5I. Fragments ejected from the surface have not been directly identified, but the fraction of the initial I removed is 2.5-fold larger than the fraction of the initial carbon removed. The retained fragments lead to desorption-limited TPD of benzene and biphenyl. These products appear from the outset of photolysis; i.e., they do not require the accumulation of intermediate species. Further, TPD after photon activation leaves C-containing fragments on the surface above the benzene and biphenyl desorption temperatures.

Mechanistically, we propose a model involving photon-activated dissociation with ejection of some I, C_6H_5, and C_6H_5I and reactions of energetic phenyl groups with neighboring species to account for TPD of C_6H_6 and $C_{12}H_{10}$.

$$C_6H_5I(a) + h\nu \rightarrow C_6H_5I^*(a) \quad (1)$$

$$C_6H_5I^*(a) \rightarrow C_6H_5I^*(g) \quad (2)$$

$$C_6H_5I^*(a) \rightarrow C_6H_5{}^*(a+g) + I^*(g \text{ and } a) \quad (3)$$

$$C_6H_5{}^*(a) + C_6H_5I \rightarrow C_{10}H_{12}(a) + I(a) \quad (4)$$

$$C_6H_5{}^* + C_6H_5I \rightarrow C_6H_6 + C_6H_4I(a) \quad (5)$$

$$C_6H_5I^*(a) \rightarrow C_6H_4(a) + HI(g) \quad (6)$$

I is an ortho−para director for electrophilic substitution reactions. Therefore, we expect H to be abstracted from either the ortho or para position in reaction 5. Positive identification of C_6H_4I has not been made. Late in the photolysis, the continued growth of C_6H_6 TPD after the $C_{10}H_{12}$ intensity has maximized may reflect the loss of neighboring C_6H_5I for reaction 4 and a shift of the source of H from C_6H_5I to any of the H-containing products including $C_{10}H_{12}$ and C_6H_4I. By comparing relative intensities, we conclude that in the early stages of photolysis the branching ratio between reaction 4 and 5 is roughly unity. Reaction 6, involving adsorbed benzyne and gas-phase hydrogen iodide, is speculatively included as an alternative I removal channel.

These results can be compared with those on LiF,[1] Ag(111),[21] and Cu(111).[20] On Cu(111), C_6H_5I dissociates thermally and forms adsorbed phenyl radicals with their π-rings tilted with respect to the surface. In TPD, reaction-limited $C_{12}H_{10}$ forms and desorbs with 100% selectivity.[26,30] On Ag(111), monolayers dissociate thermally and lead to biphenyl as on Cu(111). Irradiation of submonolayers at 248 nm led to no ejection but loss of C_6H_5I TPD peak area with a cross section of 2.7×10^{-20} cm^2, which is several orders of magnitude smaller than the gas-phase optical absorption cross section, ca. 10^{-17} cm^2. C_6H_6 was also found in postirradiation TPD. Above 2 ML and up to 100 ML, translationally hot C_6H_5 and I, but not C_6H_5I, C_6H_6, or $C_{12}H_{10}$, were found in time-of-flight spectra. On LiF, irradiation with 222 nm pulses led to desorption of translationally hot ($T > 1000$ K) I and C_6H_5 as well as 900 K C_6H_5I. No assessment of retained products was made.

The gas-phase absorption cross section for C_6H_5I at 193 nm is 6.5×10^{-17} cm^2 with a quantum yield for I of ~0.08.[18] This gives a gas-phase C−I bond cleavage cross section of 5.2×10^{-18} cm^2 compared to $(2.8 \pm 0.3) \times 10^{-18}$ cm^2 for loss of adsorbed C_6H_5I. This indicates that direct absorption can account for the observations and that Al_2O_3(0001) does not strongly quench photon-driven C_6H_5I chemistry. This stands in contrast to the strong quenching effects found for C_6H_5I photochemistry on Ag(111).[21]

Summary

C_6H_5I molecularly adsorbs on Al_2O_3(0001) at 110 K and reversibly desorbs with a peak near 187 K. Photon irradiation

(X-rays or 193 nm) induces dissociation. During irradiation, C_6H_6 and $C_{12}H_{10}$ are formed and species containing C and I are ejected. The fraction of initial I removed is 2.5 times the fraction of the initial C, suggesting, as observed on LiF and Ag(111), that I desorbs during irradiation. The TPD of C_6H_6 and $C_{12}H_{10}$ following irradiation is desorption-limited. The amount of benzene formed increases monotonically with 193 nm irradiation while biphenyl grows, saturates, and then begins to decline. These products are attributed to reactions involving energetic phenyl radicals, produced by photolysis, with neighboring C_6H_5I. Photodissociation is accounted for by direct absorption with little, as compared to Ag(111), substrate quenching.

Acknowledgment. Support of this work by the National Science Foundation (CHE9319640) and the Robert A. Welch Foundation is gratefully acknowledged.

References and Notes

(1) Villa, E.; Dagata, J. A.; Lin, M. C. *J. Chem. Phys* **1990**, *92*, 1407−1412.

(2) Zhou, X.-L.; White, J. M. *J. Chem. Phys.* **1990**, *92*, 5612−5621.

(3) Modl, A.; Domen, K.; Chuang, T. J. *Chem. Phys. Lett.* **1989**, *154*, 187.

(4) Loyd, K. G.; Roop, B.; Campion, A.; White, J. M. *Surf. Sci.* **1989**, *214*, 227.

(5) Liu, Z.-M.; Akhter, S.; Roop, B.; White, J. M. *J. Am. Chem. Soc.* **1988**, *110*, 8708−10.

(6) Fairbrother, D. H.; Trentelman, K. A.; Strupp, P.; Stair, P. C.; Weitz, E. *J. Vac. Sci. Technol. A* **1992**, *10*, 2243−47.

(7) Fairbrother, D. H.; Briggman, K. A.; Stair, P. C.; Weitz, E. *J. Chem. Phys.* **1994**, *98*, 13042−49.

(8) Marsh, E. P.; Gilton, T. L.; Meir, W.; Schneider, M. P.; Cowin, J. P. *Phys. Rev. Lett.* **1988**, *61*, 2725.

(9) Costello, S. A.; Roop, B.; Liu, Z.-M.; White, J. M. *J. Chem. Phys.* **1988**, *92*, 1019.

(10) Zhou, Y.; Feng, W. M.; Henderson, M. A.; Roop, B.; White, J. M. *J. Am. Chem. Soc.* **1988**, *110*, 4447.

(11) Okabe, H. *Photochemistry of Small Molecules*; Wiley-Interscience: New York, 1978.

(12) Calvert, J. G.; Pitts, J. N. *Photochemistry*; Wiley-Interscience: New York, 1966.

(13) Bourdon, E.; Cowin, J. P.; Harrison, I.; Polanyi, J. C.; Spencer, J.; Stanners, C. D.; Young, P. A. *J. Phys. Chem.* **1984**, *88*, 6100.

(14) Dzvonik, M.; Yang, S.; Bersohn, R. *J. Chem. Phys.* **1974**, *61*, 4408.

(15) Marconi, G. *J. Photochem.* **1979**, *11*, 385.

(16) Ichimura, T.; Mori, Y. *J. Chem. Phys.* **1973**, *58*, 288.

(17) Kawasaki, M.; Lee, S. J.; Bersohn, R. *J. Chem. Phys.* **1977**, *66*, 2647.

(18) Pence, W. H.; Baughcum, S. L.; Leone, S. R. *J. Phys. Chem.* **1981**, *85*, 3844−3851.

(19) Freedman, A.; Yang, S. C.; Kawasaki, M.; Bersohn, R. *J. Chem. Phys.* **1980**, *72*, 1028−1033.

(20) Xi, M.; Bent, B. E. *J. Am. Chem. Soc.* **1993**, *115*, 7426−7433.

(21) Szulczewski, G.; White, J. M. *Surf. Sci.* **1998**, *399*, 305−315.

(22) Zhu, X. Y.; Wolf, M.; White, J. M. *J. Chem. Phys.* **1992**, *97*, 605.

(23) Coustet, V.; Jupille, J. *Surf. Sci.* **1994**, *307−309*, 1161−1165.

(24) Pireaux, J. J.; Vermeersch, M.; Caudano, R. *J. Electron Spectrosc. Relat. Phenom.* **1992**, *59*, 33−48.

(25) *PHI−Handbook of X-ray Photoelectron Spectroscopy*; Wagner, C. D., Riggs, W. M., Davis, L. E., Moulder, J. F., Muilenberg, G. E., Eds.; Perkin-Elmer Corp.: 1979.

(26) Xi, M.; Bent, B. E. *Surf. Sci.* **1992**, *278*, 19−32.

(27) Cox, J. D.; Pilcher, G. *Thermochemistry of Organic and Organometallic Compounds*; Academic Press: New York, 1970.

(28) Garrett, S. J.; Holbert, V. P.; Stair, P. C.; Weitz, E. *J. Chem. Phys.* **1994**, *100*.

(29) Zhou, X.-L.; White, J. M. *Surf. Sci.* **1991**, *241*, 270−278.

(30) Yang, M.; Xi, M.; Hoajie, Y.; Bent, B. E.; Stevens, P.; White, J. M. *Surf. Sci.* **1995**, *341*, 9−18.